Colloids and Surfaces B: Biointerfaces
Volume 112, 1 December 2013, Pages 192–196

Synthesis of strongly green-photoluminescent graphene quantum dots for drug carrier

Zonghua Wang[a], Jianfei Xia[a], Chengfeng Zhou[a], Brian Via[b], Yanzhi Xia[a], Feifei Zhang[a], Yanhui Li[a], Linhua Xia[a], Jie Tang[c]

Show more

http://dx.doi.org/10.1016/j.colsurfb.2013.07.025

Highlights

- A novel approach for preparing strongly fluorescent graphene quantum dots has been developed.
- We first use periodic acid as an oxidant to prepare GQDs-PEG and get good results.
- The photoluminescence (PL) quantum yield of the GQDs-PEG was about 18.8%.
- GQDs-PEG possess high loading capability (2.5 mg/mg).

Abstract

A novel approach has been developed for the preparation of strongly green-photoluminescent graphene quantum dots (GQDs-PEG) which have been surface-passivated by polyethylene glycol. The photoluminescence (PL) quantum yield of the GQDs-PEG with 400 nm excitation was about 18.8%, which was higher than other GQDs reported in the literature. More importantly, the surface-passivated PEG on GQDs can not only enhance PL intensity but also load drug by hydrogen bonding. Moreover, the high specific surface area of GQDs-PEG endowed them high loading capability (2.5 mg/mg) to carry drug. The results demonstrated that the GQDs-PEG were suitable for drug carrier and cell imaging.

Graphical abstract

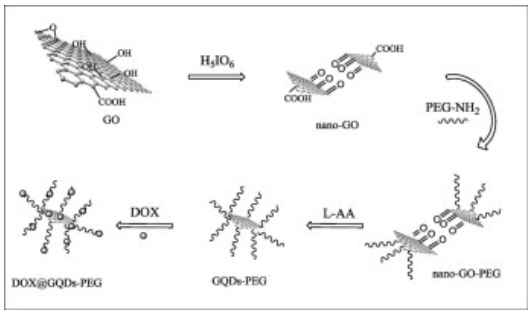

Figure options

Keywords

Graphene quantum dots; Polyethylene glycol; Surface passivation; Photoluminescence; Drug carrier

1. Introduction

Graphene, a two-dimensional nanomaterial that was reported for the first time in 2004 [1,2], has been widely investigated because of its novel physical properties and potential applications in nanoelectronic devices [3], energy storage and conversion [4,5], biotechnology [[6], [7] and [8]], nanocomposite materials [9,10]. Recently, several research groups have explored graphene for biomedical applications,

such as drug loading and delivery [11,12]. However, one critical problem lies in the ability to trace the dynamic route of graphene in cells and observe whether it is cleared off quickly by cells or stays for a period of time. For this purpose, graphene must possess concurrent signals that allow for the rapid monitoring of the drug route so that the behaviors within the organism can be accurately identified. Therefore, a fascinating topic is how to make the graphene give off some measurable signals, for example, photoluminescence in optical imaging. Due to high resistance to photobleaching, narrow emission spectra, broad excitation spectra and long fluorescence lifetime, quantum dots (QDs) could be used as a potential luminescence probes [[13], [14], [15], [16], [17] and [18]]. However, potential heavy metal toxicity as a result of leakage constituent ions (e.g., cadmium, mercury, lead, etc.) is still a problem [19].

To solve the above problems, graphene quantum dots (GQDs), a new kind of nanomaterial with the combined properties of graphene and QDs are considered as natural candidate for effective drug delivery. First of all, the high specific surface area and biocompatibility endows their capability to load drugs efficiently with lower toxicity. Also importantly, due to the PL of GQDs, the delivery complex can be observed without further modifying them with other marker dyes.

Until now, a series of methods have been developed to obtain GQDs [[20], [21], [22] and [23]]. However, current synthetic methods are still have deficiencies in strict requirement for special equipment, precise controlling lateral dimensions as well as obtaining high quantum yields. It is apparent that more effective methods for GQDs preparation are needed. In addition, due to their specifical application in optical bioimaging, the stronger fluorescence is needed. A particular interest and significance was the recent finding that small carbon nanoparticles could be surface-passivated by organic molecules to become strongly fluorescent in the visible and near-infrared spectral regions. Many organic polymers could be used to enhance the surface passivation of GQDs. For example, diamine-terminated oligomeric poly(ethylene glycol) (PEG1500N) and poly(propionylethyleneimine-co-ethyleneimine) (PPEI-EI) were used to react with the carbon dots to enhance fluorescence [24].

In this paper, we present a novel method for the synthesis of high intensity green-photoluminescent GQDs-PEG. Our preparation method requires no elaborate equipment and is based on the tailoring of graphene oxide (GO) [25] by periodic acid in a mild condition followed by the reduction of nano-GO with L-ascorbic acid (L-AA) and then surface-passivated by PEG-NH_2 to produce photoluminescent GQDs-PEG. The prepared GQDs-PEG possess PL quantum yields as high as 18.8%, which is higher than the other GQDs (5–13%) [26]. Also, the obtained GQDs-PEG show size-dependent photoluminescent, which could be supported by the previous report [27]. It will be shown that surface-passivation by PEG not only enhances the fluorescence but also improves the solubility of the GQDs. In addition, the reducing agent used in this research is not hydrazine hydrate, widely used in the preparation of GODs [28], but L-ascorbic acid, a kind of endogenous metabolites. So our preparation method is green, and the obtained GQDs-PEG have good biocompatibility, which is more suitable for the application as drug carrier. Due to the stable photoluminescence, low cytotoxicity, excellent solubility and biocompatibility, the GQDs-PEG is demonstrated to be an efficient drug carrier with tracking capability.

2. Experimental details

2.1. Synthesis of GQDs-PEG

All chemicals and reagents used for the experiments were analytical grade and purchased from the Hefei Bomei Biotechnology Co. Ltd., China. Firstly, GO was synthesized from expandable graphite using a modified Hummers method [29]. Then 15 g periodic acid were added into 10 mL GO dispersion at a concentration of 3 mg/mL and the mixed solution was kept at 60 °C for 24 h. The precipitate was centrifuged and washed with deionized water until the supernatant was neutral. Secondly, 2-morpholinoethane sulfonic acid monohydrate (MES) (0.25 mmol), N-(3-dimethylaminopropyl)-N′-ethyl-carbodiimide hydrochloride (EDC) (0.5 mmol) and N-hydroxysuccinimide (NHS) (0.5 mmol) were added into 10 mL the above nano-GO solution (concentration is 2 mg/mL) and ultrasonically vibrated for 1 h then stirred overnight. The pH of the reaction solution was adjusted to approximate 9.0 by dropping in 100 μL triethylamine, then 0.05 mmol poly(propylene glycol)-block-poly(ethylene glycol)-block-poly(propylene glycol) bis(2-aminopropyl ether) (PEG-NH_2, Mw = 900) was added into the reaction mixture and it was stirred for 4 days at room temperature. After the conjugation reaction, the suspension was ultra-centrifuged and the precipitates were washed with distilled water, with several ultra-centrifugation and re-dispersion cycles over several days. Later on, the obtained nano-GO-PEG was dispersed in 10 mL distilled water. L-AA (200 mg) was added into the aqueous solution and stirred at 50 °C for 24 h; and the nano-GO-PEG was reduced to GQDs-PEG. Finally, the resulted suspension was dialyzed in a dialysis bag (retained molecular weight: 3500 Da) overnight and GQDs-PEG with strongly fluorescent were obtained. As comparison, the GQDs without PEG were prepared using the same methods above.

2.2. Quantum yields (QY) measurements

9,10-Bis(phenylethynyl) anthracene in cyclohexane (QY = 1) were chosen as standards. The quantum yields of GQDs-PEG (in water) were calculated according to:

Turn MathJax on

where Φ is the quantum yield, I is the measured integrated emission intensity, η is the refractive index of the solvent, and A is the optical density. The subscript "st" refers to a standard with known quantum yield and "x" for the sample. In order to minimize re-absorption effects, absorption in the 10 mm fluorescence cuvette was kept below 0.10 at the excitation wavelength (400 nm).

2.3. pH-dependent doxorubicin (DOX) loading and release from GQDs-PEG

The preparation process of DOX@GQDs-PEG is shown in Scheme 1. GQDs-PEG and DOX with the final concentration of 0.1 mg/mL and 0.5 mg/mL were first ultrasonically vibrated with phosphate buffer solution (PBS) at different pH (pH = 5.5, 7.4 and 9.0), and then stirred for 24 h at room temperature in the dark and then ultra-centrifuged. To evaluate the DOX loading efficiency, the DOX concentration in the upper layer was measured using a standard DOX concentration curve generated using the UV–vis spectrophotometer from a series of DOX solutions with different concentrations. The nanohybrids DOX@GQDs-PEG (3 mg) were dispersed in 3 mL of aqueous solution and the dispersion was divided into three equal aliquots. The DOX@GQDs-PEG samples used for the release experiments were placed into dialysis bags, which were dialyzed in 60 mL of PBS buffer solution with pH 5.5, 7.4, and 9.0, respectively. The drug release was assumed to start as soon as the dialysis bags were placed into the reservoir. The release reservoir was kept under constant stirring. One of the dialysis bags was taken out for characterization at various time intervals. The concentration of DOX released from DOX@GQDs-PEG was quantified using UV–vis spectroscopy.

Scheme 1.

The sketch map for the preparation of DOX@GQDs-PEG.

Figure options

2.4. Characterization

Transmission Electron Microscope (TEM) observations were performed on a JEM-2100F electron microscope. Fourier Transform Infrared (FTIR) spectra were recorded with a Perkin-Elmer-283B FTIR spectrometer within the wave range 750–4000 cm^{-1}. Ultraviolet visible (UV–vis) absorption and fluorescence spectra were recorded at room temperature on a Hitachi 3100 spectrophotometer and an F-96 spectrophotometer, respectively.

3. Results and discussion

Fig. 1 shows typical TEM images of the pristine GO and the GQDs-PEG. Before the periodic acid treatment, the GO is flake-like shape (Fig. 1(a)). After the oxidization and reduction treatment, the GQDs-PEG was formed, resulting in small particles. By the present method, the as-prepared GQDs-PEG are homogeneous with a mean diameter of ca. 15 nm (Fig. 1(b)).

Fig. 1.

TEM images of (a) the pristine GO and (b) GQDs-PEG, the inset is the diameter distribution of the GQDs-PEG.

Figure options

From the FTIR spectra of GO (Fig. 2(a)), oxygen-containing functional groups were introduced as evidenced by the peak at C

O/COOH (1720 cm^{-1}), OH (3430 cm^{-1}), and COC (1097 cm^{-1}). The surface-passivation and deoxidization was further confirmed by the changes in the FTIR (Fig. 2(b)). The FTIR absorbance peaks of GQDs-PEG at 1735 cm^{-1} (CO) and 1580 cm^{-1} (NH) indicated the formation of amido bond between GQDs and PEG. At the same time, the peaks at ~2885 cm^{-1} and ~1106 cm^{-1} in GQDs-PEG sample were associated with CH bond and CO bond in PEG, which suggested that the PEG was successfully conjugated with the GQDs. Also, the strongest vibrational absorption band of CO/COOH at 1720 cm^{-1} subsided, which confirmed the reduction of GO.

Fig. 2.

FTIR spectra of (a) GO and (b) GQDs-PEG.

Figure options

The UV–vis absorption spectrum of GQDs-PEG in water shows an absorption band at ca. 320 nm, which is similar to the reported GQDs [30,31]. However, different to that of blue-luminescent hydrothermally synthesized GQDs, the synthesized GQDs-PEG excited by 400 nm lamp emitted green luminescence (Fig. 3, inset), which was probably attributable to the size effect.

Fig. 3.

UV–vis absorption of GQDs-PEG. Inset: photograph of the GQDs-PEG excited by 400 nm lamp.

Figure options

To further explore the optical properties of as-synthesized GQDs-PEG, a detailed PL study was carried out. As shown in Fig. 4, the emission spectra of the as-prepared GQDs-PEG showed an excitation-dependent feature, which is similar to the GQDs synthesized with hydrothermal method [30]. For the excitation near the absorption band of 400 nm, GQDs-PEG showed a strongest peak at 518 nm (Fig. 4(a)). When PEG was omitted, a similar excitation-dependent feature was also observed on GQDs, but all of the non-passivated particles expressed weaker PL (Fig. 4(b)). Therefore, this phenomenon could be explained that the improvement of PL intensity is attributed to the effect of PEG.

Fig. 4.

Fluorescence spectra of GQDs-PEG (a) and GQDs (b) using different excitation wavelengths.

Figure options

Using 9,10-bis(phenylethynyl) anthracene as a reference, the PL quantum yield of GQDs-PEG was measured to be 18.8% (Table 1), which is higher than that of reported GQDs (5–13%) [26]. Generally speaking, the PL of GQDs has been tentatively suggested to arise from excitons of carbon, emissive traps, quantum-confinement effect, aromatic structures, free zig-zag sites and/or edge defects. For the PL mechanism of GQDs-PEG, it is speculated that both the quantum size effect and surface defects contribute to PL. Each GQD has some defects due to the reduction process, and after passivated with PEG, the presence of surface energy traps that become emissive upon stabilization. However, a widely accepted mechanism for luminescence from GQDs-PEG remains unavailable and needs further investigation.

Table 1.

Quantum yield of GQDs-PEG using 9,10-bis(phenylethynyl) anthracene as a reference. Error bars represent the standard deviation of the data (n = 3).

Sample	Integrated emission intensity (I)	Abs. at 400 nm (A)	Refractive index of solvent (η)	Quantum yield (Φ)
9,10-Bis(phenylethynyl) anthracene	19873.5 ± 99.6	0.067 ± 0.0008	1.43	1 (known)
GQDs-PEG	3423.6 ± 41.1	0.053 ± 0.0009	1.33	0.188 ± 0.003

Table options

To evaluate the potential of GQDs-PEG as a nano-carrier for drug delivery, a water-soluble anti-cancer drug DOX was chosen for investigation. Fig. 5(a) shows the loading of DOX on GQDs-PEG at the initial DOX concentration of 0.5 mg/mL at pH values of 5.5, 7.4 and 9, respectively. As expected, the GQDs-PEG showed distinctly different loading capacities toward DOX at different pH values. The maximum loading capacity of DOX on GQDs-PEG is 0.9 mg/mg at pH 5.5, 2.5 mg/mg at pH 7.4, and 1.1 mg/mg at pH 9. The highest loading capacity is observed at the neutral condition, rather than acidic or alkaline conditions. The release of drug from the drug carrier depends on various experimental factors such as pH, degradation rate, particle size and interaction between drug and drug carrier. Herein, the release behavior of DOX from GQDs-PEG is shown in Fig. 5(b). DOX releases slowly from GQDs-PEG and the release rate gradually declines after 9 h. In the first 48 h under neutral conditions (pH 7.4), about 37% of the total bound DOX was released from the nanohybrid. The release behavior under acidic and alkaline conditions indicates that 75% and 51% of the total bound DOX were released from the nanohybrid after 48 h at pH 5.5 and 9.0, respectively, which is much higher than that under neutral conditions. At a lower pH, the increased hydrophilicity and higher solubility of DOX were caused by increased protonation of NH_2 groups on DOX, thereby reducing the hydrophobic interaction between DOX and GQDs-PEG. It was a critical factor since the DOX-loaded nanocomposite was expected to be released prevailingly around the tumor (pH 5–6) sites due to their acidic environment. Therefore, the DOX@GQDs-PEG nanocomposite highlights its anti-cancer efficacy by reducing the pre-release of DOX before the uptake by the targeting cell and enhancing the controlled-release capability for drug delivery.

Fig. 5.

The loading capacity (a) and the release rate (b) of DOX on DOX@GQDs-PEG at different pH values. Error bars represent the standard deviation of the data (n = 3).

Figure options

4. Conclusions

In conclusion, strongly green fluorescent GQDs-PEG with PL quantum yields as high as 18.8% have been prepared. The PL intensity of GQDs-PEG is further improved by surface-passivated with polyethylene glycol. Due to the inherent PL and high drug loading capability (2.5 mg/mg), GQDs-PEG are demonstrated to be a good candidate for drug carrier without further modification.

Acknowledgements

This work was financially supported by the National Natural Science Foundation of China (authorization numbers: 20975056, 21275082 and 81102411); the Natural Science Foundation of Shandong (ZR2011BZ004, ZR2011BQ005); JSPS and NSFC under the Japan-China Scientific Cooperation Program (21111140014); the State Key Laboratory of Analytical Chemistry for Life Science (SKLACLS1110); and the National Key Basic Research Development Program of China (973 special preliminary study plan, Grant no.: 2012CB722705).

References

[1]
A.K. Geim, K.S. Novoselov
Nat. Mater., 6 (2007), p. 183
Loading

[2]
A.H.C. Neto, F. Guinea, N.M.R. Peres, K.S. Novoselov, A.K. Geim
Rev. Mod. Phys., 81 (2009), p. 109
Loading

[3]
F. Liu, S. Song, D. Xue, H. Zhang
Adv. Mater., 24 (2012), p. 1089
Loading

[4]
C. Liu, J. Liu, S. Ji, Y. Zhou
Mater. Focus, 1 (2012), p. 149
Loading

[5]
F. Liu, J. Liu, D. Xue
Mater. Focus, 1 (2012), p. 160
Loading

[6]
D. Chen, J.H. Li
Chem. Rev., 112 (2012), p. 6027
Loading

[7]
L.H. Tang, Y. Wang, Y. Liu, J.H. Li
ACS Nano, 5 (2011), p. 3817
Loading

[8]
Y. Wang, Z.H. Li, J.H. Li, Y.H. Lin
Trends Biotechnol., 29 (2011), p. 205
Loading

[9]
Y. Wang, Z.H. Li, D.H. Hu, C.T. Lin, J.H. Li, Y.H. Lin
J. Am. Chem. Soc., 132 (2010), p. 9274
Loading

[10]
H. Wu, W. Chen
Mater. Focus, 1 (2012), p. 116
Loading

[11]
X. Sun, Z. Liu, K. Welsher, J. Robinson, A. Goodwin, S. Zaric, H. Dai
Nano Res., 1 (2008), p. 203
Loading

[12]
Z. Liu, J.T. Robinson, X. Sun, H. Dai
J. Am. Chem. Soc., 130 (2008), p. 10876
Loading

[13]
P. Huang, J. Lin, Z. Li, H. Hu, K. Wang, G. Gao, R. He, D.X. Cui
Chem. Commun., 46 (2010), p. 4800
Loading

[14]
Y. Wang, J. Lu, L.H. Tang, H.X. Chang, J.H. Li
Anal. Chem., 81 (2009), p. 9710
Loading

[15]
C. Zhang, K. Li, D. Xue
Mater. Focus, 1 (2012), p. 45
Loading

[16]
X. Gao, L. Yang, J. Petros, F. Marshall, J. Simons, S. Nie
Curr. Opin. Biotechnol., 16 (2005), p. 63
Loading

[17]
C.X. Song, Y. Zhang, L.H. Jiang, D.B. Wang
Sci. Adv. Mater., 4 (2012), p. 1096
Loading

[18]
C.B. Zhang, K.Y. Li, S.Y. Song, D.F. Xue
Sci. Adv. Mater., 4 (2012), p. 1148
Loading

[19]
R. Hardman
Environ. Health Perspect., 114 (2006), p. 165
Loading

[20]
L.A. Ponomarenko, F. Schedin, M.I. Katsnelson, R. Yang, E.W. Hill, K.S. Novoselov, A.K. Geim
Science, 320 (2008), p. 356
Loading

[21]
V. Gupta, N. Chaudhary, R. Srivastava, G.D. Sharma, R. Bhardwaj, S. Chand
J. Am. Chem. Soc., 133 (2011), p. 9960
Loading

[22]
J.H. Shen, Y.H. Zhu, C. Chen, X.L. Yang, C.Z. Li
Chem. Commun., 47 (2011), p. 2580
Loading

[23]
Y. Li, Y. Hu, Y. Zhao, G.Q. Shi, L.E. Deng, Y.B. Hou, L.T. Qu

Adv. Mater., 23 (2011), p. 776

Loading

[24]

Y.P. Sun, B. Zhou, Y. Lin, W. Wang, K.A. Shiral Fernando, P. Pathak, M.J. Meziani, B.A. Harruff, X. Wang, H. Wang, P.G. Luo, H. Yang, M.E. Kose, B. Chen, L.M. Veca, S.Y. Xie

J. Am. Chem. Soc., 128 (2006), p. 7756

Loading

[25]

D. Chen, H.B. Feng, J.H. Li

Chem. Rev., 112 (2012), p. 6027

Loading

[26]

S.J. Zhu, S.J. Tang, J.H. Zhang, B. Yang

Chem. Commun., 48 (2012), p. 4527

Loading

[27]

S. Kim, S.W. Hwang, M.K. Kim, D.Y. Shin, C.O. Kim, S.B. Yang, J.H. Park, E. Hwang, S.H. Choi, G. Ko, S. Sim, C. Sone, H.J. Choi, S. Bae, B.H. Hong

ACS Nano, 6 (2012), p. 8203

Loading

[28]

J.H. Shen, Y.H. Zhu, X.L. Yang, J. Zong, J.M. Zhang, C.Z. Li

New J. Chem., 36 (2012), p. 97

Loading

[29]

C.F. Zhou, Z.H. Wang, J.F. Xia, B.K. Via, F.F. Zhang, Y.Z. Xia, Y.H. Li

C. R. Chim., 15 (2012), p. 714

Loading

[30]

D.Y. Pan, J.C. Zhang, Z. Li, M.H. Wu

Adv. Mater., 22 (2010), p. 734

Loading

[31]

Y. Li, Y. Hu, Y. Zhao, G. Shi, L. Deng, Y. Hou, L. Qu

Adv. Mater., 23 (2011), p. 776

Loading

- Corresponding author at: Department of Chemistry, College of Chemistry, Chemical Engineering and Environment, Qingdao University, Qingdao 266071, PR China. Tel.: +86 532 85950873; fax: +86 532 85950873.
- Corresponding author at: College of Chemistry, Chemical Engineering and Environment, Qingdao University, Qingdao 266071, PR China.

View more articles »

Citing articles (0)

Related reference work articles